Hindawi Publishing Corporation
Science and Technology of Nuclear Installations
Volume 2015, Article ID 652731, 6 pages
http://dx.doi.org/10.1155/2015/652731

Research Article

Analysis of Wetting Characteristics on Microstructured Hydrophobic Surfaces for the Passive Containment Cooling System

Wei Zhao, Xiang Zhang, Chunlai Tian, and Zhan Gao

State Nuclear Power Technology Research & Development Center, Beijing 102209, China

Correspondence should be addressed to Wei Zhao; zhaowei@snptrd.com

Received 15 January 2015; Revised 25 May 2015; Accepted 2 June 2015

Academic Editor: Massimo Zucchetti

As the heat transfer surface in the passive containment cooling system, the anticorrosion coating (AC) of steel containment vessel (CV) must meet the requirements on heat transfer performance. One of the wall surface ACs with simple structure, high mechanical strength, and well hydrophobic characteristics, which is conductive to form dropwise condensation, is significant for the heat removal of the CV. In this paper, the grooved structures on silicon wafers by lithographic methods are systematically prepared to investigate the effects of microstructures on the hydrophobic property of the surfaces. The results show that the hydrophobicity is dramatically improved in comparison with the conventional Wenzel and Cassie-Baxter model. In addition, the experimental results are successfully explained by the interface state effect. As a consequence, it is indicated that favorable hydrophobicity can be obtained even if the surface is with lower roughness and without any chemical modifications, which provides feasible solutions for improving the heat transfer performance of CV.

1. Introduction

The advanced pressurized water reactor [1] adopts a passive containment cooling system [2, 3] (PCCS) relying on heat removal by condensation to maintain the steel containment vessel (CV) within the design limits of pressure and temperature, which effectively prevents the leakage of radioactive materials under accident situations. As the condensation surface in PCCS, the safety-related anticorrosion coating (AC) of CV must meet the requirements of heat removal capacity. The thermal conductivity of current applicative coating on CV is about 1.0 $Wm^{-1}K^{-1}$; besides the thickness of the coating is in the range of 50–150 μm, which results in high thermal resistance. Meanwhile, the contact angle of the coating is lower than 30°; such high wettability results in filmwise condensation [4]. Compared with filmwise condensation, heat transfer coefficients for dropwise condensation of steam are greater with one to two orders of magnitude [5–9], which can effectively enhance the ability of heat transfer on CV, while dropwise condensation takes place on a hydrophobic surface where the contact angle is usually larger than 90 degrees, whose heat transfer rate increased with the increase in the contact angle [10]. Therefore, for further improving the running safety of the existing or future high-power nuclear power plant, the lower thermal resistance, simple structure, excellent physical and chemical stability, and optimized hydrophobic surface are highly in demand for the safety margin of CV.

Si is one of the particularly promising coating materials because of low cost [11], higher thermal conductivity [12], favorable chemical stability [13], and mature processing technologies. Therefore, as the coating material, Si has great advantages in the heat transfer requirements of CV. In the present work, the grooved structures in different sizes on silicon wafers by lithographic methods are systematically prepared to investigate the effects of microstructures on the hydrophobic property of the surfaces. The results demonstrate that outstanding hydrophobic performance can be

obtained by microstructure engineering without any chemical modifications; the mechanism of hydrophobic enhancement is described and discussed as well.

2. Materials and Methods

2.1. Fabrication. Si wafers ($1 \times 1\,cm^2$) were grooved to form a groove pattern structure of width "a" and spacing "b." Substrates with different combinations (a and b) were used in the present study. Hereinafter, these patterns were referred to as "width/spacing." Patterns were etched into silicon wafers using standard photolithography techniques. The samples were spin coated with a positive photoresist (Shipley S1813) at 4000 r/min for 60 s (1.5 μm thick coating). After a preexposure bake at 115°C for 3 min, the wafers were exposed in the ultraviolet (Karl Suss) for 18 s with the desired pattern. After a postexposure bake at 110°C for 10 min, the samples were developed in Microposit 351 for 30 s and rinsed with deionized water. The silicon was then dry-etched using ICP (Oxford Plasmalab System100 ICP180) with O_2 and SF_6 at an etch rate of 110 μm/h. Meanwhile, the etching heights were controlled by managing the etching time.

2.2. Characterization Methods. The microstructure was observed and evaluated on a scanning electron microscope (SEM, FEI nova 430) and a profilometer (Bruker DektakXT). The surface contact angles (CAs) on the fabricated substrates were determined using a CA measurement system (Kruss DSA 100). Using a deionized water droplet of about 5 μL at room temperature, an average of static CAs measured at three different locations were used for presentation.

3. Results and Discussion

Figure 1 shows the SEM images of the grooved surface prepared using a photomask (width/spacing ratio = 1:1 and with approximate heights of 5 μm). It is obvious that the surface is uniform and the structural integrity is not violated. The measurement results show that the dimensions of width/spacing are 40/40, 60/60, 90/90, 120/120, and 150/150 μm, respectively.

The wetting behavior of solid surfaces by a liquid is usually expressed by the CA [14]. The CA concept is of fundamental importance in all solid-liquid-fluid interfacial phenomena [15, 16]. In this work, when the width/space is 40/40 μm, the CA is 132°, and the CAs decrease as the dimension of width/spacing increases. When the dimension of width/spacing reaches 150/150 μm, the CA decreases to 122°, and the values of CAs are summarized in Table 1.

At present, two wetting models are successively proposed to describe the relationship between surface roughness and the apparent contact angle of a solid surface: Wenzel [17, 18] and Cassie-Baxter [19] models. The basic assumption in the Wenzel model (a noncomposite state) is that liquids completely fill the grooves of rough surfaces. And the Wenzel model can be expressed by the following equation [17]:

$$\cos\theta_w = r\cos\theta_s, \tag{1}$$

Table 1: The characteristics of prepared grooved surface: width a, spacing b, roughness factor r, apparent CAs in the Wenzel model θ_w, fraction f_s, apparent CAs in the Cassie-Baxter model θ_c, and the measurement results of CAs $\theta_{r/h5}$ ($h = 5\,\mu$m).

a (μm)	b (μm)	r	θ_w (°)	f_s	θ_c (°)	$\theta_{r/h5}$ (°)
40	40	1.13	66.8	0.5	109.0	132.0
60	60	1.08	67.7	0.5	109.0	130.0
90	90	1.06	68.3	0.5	109.0	126.5
120	120	1.04	68.6	0.5	109.0	126.0
150	150	1.03	68.8	0.5	109.0	122.0

where θ_w is the apparent contact angle in the Wenzel state, θ_s is Young's contact angle [20], and r is the surface roughness factor, the ratio between the actual surface area and the apparent surface area of a rough surface. The Wenzel equation predicts that surface roughness enhances both hydrophilicity and hydrophobicity, which is dependent on the nature of the corresponding surface. If the surface roughness factor is larger than 1, a hydrophilic surface becomes more hydrophilicity with the increase in surface roughness [21]. Conversely, a hydrophobic surface will present increased hydrophobicity.

Cassie-Baxter model [19] is proposed to clarify the relationship between chemical heterogeneities and the contact angle. The basic assumption in the Cassie-Baxter model (a composite state) is that liquids only contact the top of solid asperities, and air pockets are presumed to be trapped underneath the liquid. The Cassie-Baxter model can be expressed by the following equation [19]:

$$\cos\theta_c = f_s\cos\theta_s + (1 - f_s)\cos\theta_v, \tag{2}$$

where f_s is the fraction of the liquid base in contact with the solid surface, $f_s < 1$, and $(1 - f_s)$ is the fraction of the liquid base in contact with air pockets. θ_c is apparent contact angles in the Cassie-Baxter model. In this case, θ_s and θ_v are Young's contact angles corresponding to the two components, that is, solid and air. Air is not able to be wetted by water; therefore the water/air CA equals 180°; what is more the cosine of the CA is –1. The Cassie-Baxter equation can be derived as

$$\cos\theta_c = f_s\cos\theta_s + f_s - 1. \tag{3}$$

In our case, the surface roughness factor and the fraction are defined as $r = (a + b + h)/(a + b)$ and $f_s = a/(a + b)$, respectively, due to the parallel grooved surface. In addition, θ_s is 69.5° achieved by the measurement of intrinsic Si without grooved surface; then the apparent contact angles θ_w in the Wenzel model and θ_c in the Cassie-Baxter model can be obtained from (1) and (3); the calculated results are summarized in Table 1.

As can be seen from Table 1, according to the Wenzel model, the apparent CAs θ_w (calculated value) are lower than those of θ_s. On the other hand, the apparent CAs θ_c, calculated by Cassie-Baxter model, are larger than those of θ_s. In addition, based on the Cassie-Baxter model, even if a and b are increased from 40 μm to 150 μm, f_s is constant of 0.5 due to the constant width/spacing ratio, and its corresponding

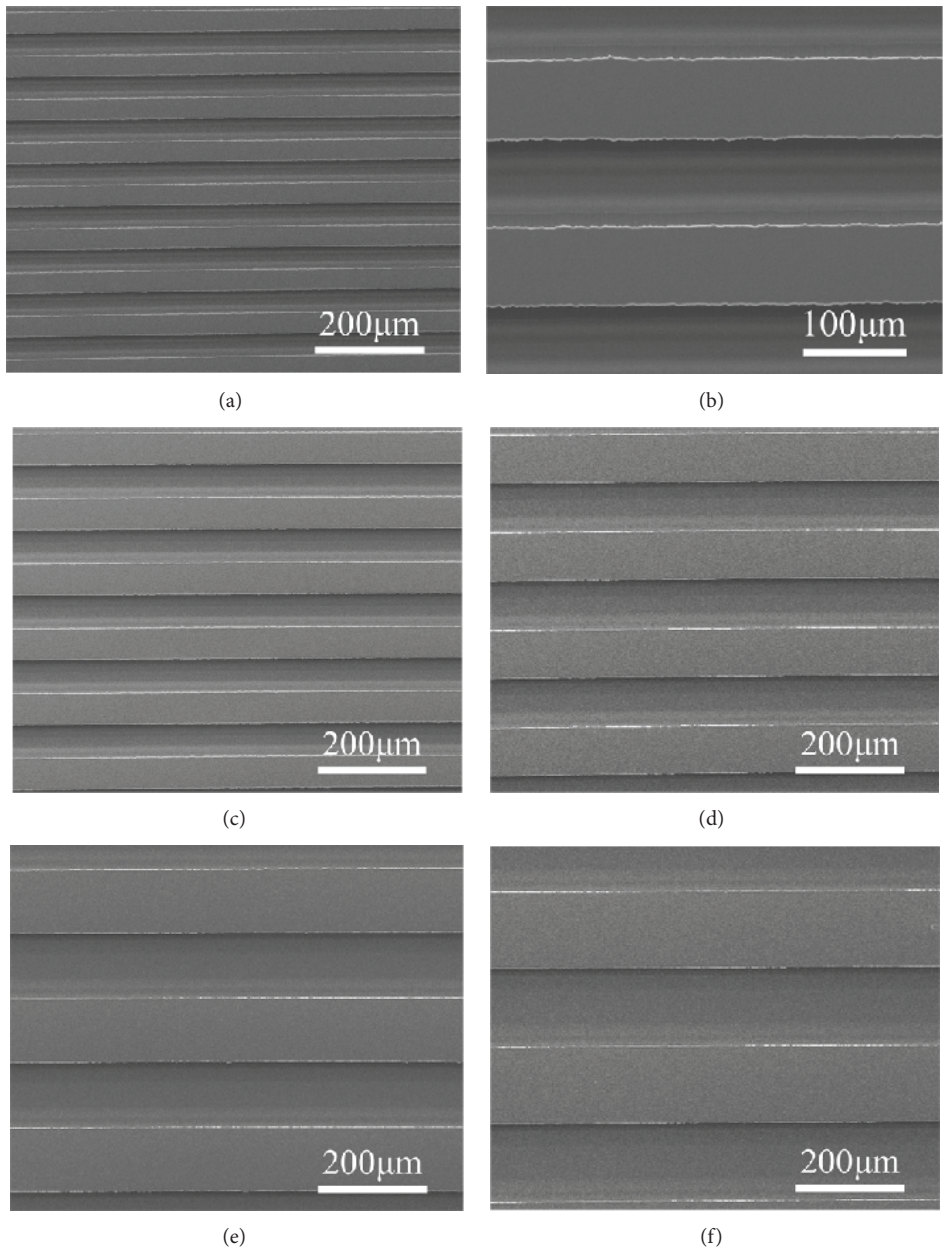

FIGURE 1: SEM images of grooved patterned Si substrate ($h = 5\ \mu$m) of (a) 40/40 μm, (b) high-magnification image of 40/40 μm, (c) 60/60 μm, (d) 90/90 μm, (e) 120/120 μm, and (f) 150/150 μm.

calculated apparent CAs θ_c values keep the constant of 109°. However, the measurement results of CAs θ_r show $\theta_{r/h5}$ in the range of 122° to 132°; that is, both the conventional Wenzel model (a noncomposite state) and Cassie-Baxter model (a composite state) underestimate the CAs.

Herein, considering that the noncomposite contact tends to form hydrophilic surface, whereas composite contact tends to arrive at hydrophobic surface, it is reasonable to assume that the wetting behavior of grooved surface belongs to composite state. In order to verify and validate the above analysis, two series of grooved surface with etching height h of 15 μm and 50 μm are prepared on Si wafers by controlling the etching time. As can be seen from Table 2, the measurement results show that both the CAs of $\theta_{r/h15}$ and $\theta_{r/h50}$ decrease from ~134° to ~120° as the dimension of width/spacing increases from 40 μm to 150 μm, which is consistent with the measurement results of $\theta_{r/h5}$. It is indicated that the CAs are independent of the groove height and the droplet tends to sit on the grooved surfaces, whose behavior is consistent with that described in the Cassie-Baxter model.

Based on the above experimental results, it is demonstrated that the system is attributed to the composite state; that is, the water droplet rests on the surface without penetration. However, it is important to note that, when compared

Table 2: The characteristics of prepared grooved surface: width a, spacing b, the measurement results of CA with 15 μm height $\theta_{r/h15}$ and 50 μm height $\theta_{r/h50}$.

a (μm)	b (μm)	$\theta_{r/h15}$ (°)	$\theta_{r/h50}$ (°)
40	40	135.0	133.0
60	60	132.0	129.0
90	90	131.0	130.0
120	120	131.0	125.5
150	150	121.5	118.0

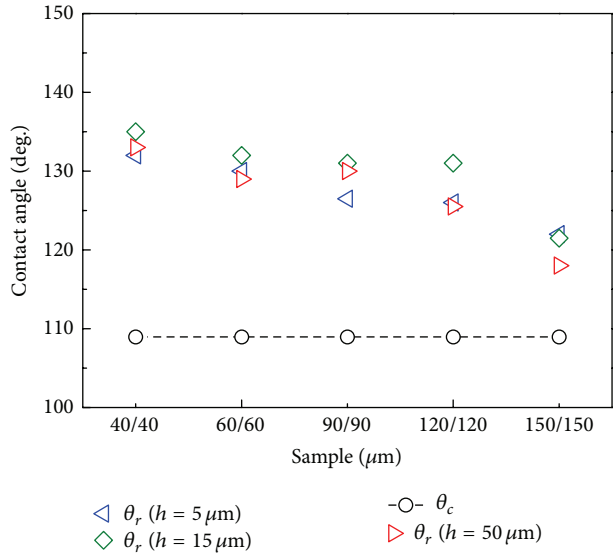

Figure 2: Effect of groove size (a and b) for constant width/spacing ratio. Dashed line denotes the CAs calculated from Cassie-Baxter model.

with θ_c calculated from Cassie-Baxter equation (dashed line in Figure 2), the measurement value θ_r still exhibits significantly distinct features; that is, conventional Cassie-Baxter model underestimates the CAs 15–25°. It is suggested that the composite state is different from the conventional Cassie-Baxter model. By further analysis, such obvious distinction is originated from the formation of interface states effect in grooved surface, which will be discussed below.

As shown in Figure 3(a), at the interface of liquid and solid, an air bubble is found besides the conventional air pocket. Furthermore, different etching height h of the sample also has the extra air bubble, which implies that such phenomenon is repeatable. As a result, a semiquantitative reinforced Cassie-Baxter model via the formation of air bubbles is proposed to explain the dramatically improved hydrophobic properties. As shown in Figures 3(b) and 3(c), on the basis of Cassie-Baxter model, extra air bubbles are trapped beneath the liquid. In such a case the liquid contact with the solid surface is greatly reduced. Therefore, the corresponding apparent CAs are considerably enhanced. In addition, the contact area reduced by air bubble can be calculated from (3). For instance, for the microstructure of 120/120 μm, substituting the measured θ_r and Young's contact angle of Si θ_s into (3), it is easy to calculate that the fraction f_s equals 0.3, which is lower than the theoretical value 0.5. It is intensely demonstrated that the existence of bubble reduces the contact area between liquid and solid by 40 percent on the basis of conventional Cassie-Baxter model. It is also indicated that excellent hydrophobicity properties can be achieved, even if the surface is without chemical modifications, which provides a feasible solution for improving the heat transfer performance of CV in PCCS. In order to obtain deeper insight into interface states, more work will be carried out by experimental and theoretical study in the future.

4. Conclusions

The grooved structures on silicon wafers by lithographic methods are systematically fabricated to investigate the effects of microstructures on the hydrophobic property of the surfaces, and the hydrophobic performance of Si surface is optimized by microstructure manufacturing. A strong correlation between the microstructure and hydrophobic characteristics of grooved surface is obtained. The mechanism of hydrophobic enhancement is successfully explained and discussed by the interface state effect. Based on the results of this study, the following conclusions can be made:

(1) The hydrophobicity is dramatically enhanced in comparison with the conventional Wenzel or Cassie-Baxter models; specifically the measurement results

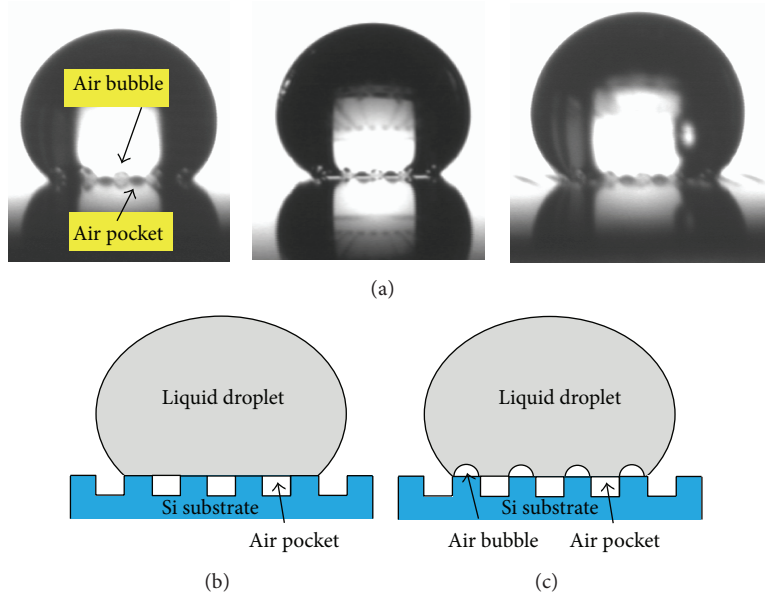

FIGURE 3: (a) Morphologies of water droplets on prepared grooved surfaces (120/120 μm) with height of 5 μm, 15 μm, and 50 μm, (b) schematic of the Cassie-Baxter model, and (c) reinforced Cassie-Baxter model.

of CAs are dramatically enhanced nearly 25° compared with the apparent CAs which are calculated by Cassie-Baxter model.

(2) Effect on interface states is proposed to explain this phenomenon; the enhanced hydrophobicity is mainly attributed to the formation of extra air bubbles at the solid-liquid interface. Such results provide insight into the design and optimization of the high-efficiency heat transfer surface of CV.

(3) Favorable hydrophobicity can be obtained even if the surface is with lower roughness and without any chemical modifications, which provides feasible solutions for improving the heat transfer performance of CV. Furthermore, the hydrophobicity performance can be further improved by chemical modification to reduce the surface free energy, which should take more time and effort to study in the near future.

Conflict of Interests

The authors declare that they have no conflict of interests regarding the publication of this paper.

Acknowledgment

The work is supported by the Staff Independent Innovation Fund of SNPTC (State Nuclear Power Technology Company, China) with Grant no. SNP-KJ-CX-2013-9.

References

[1] T. L. Schulz, "Westinghouse AP1000 advanced passive plant," *Nuclear Engineering and Design*, vol. 236, no. 14–16, pp. 1547–1557, 2006.

[2] W. T. Sha, T. H. Chien, J. G. Sun, and B. T. Chao, "Analysis of large-scale tests for AP-600 passive containment cooling system," *Nuclear Engineering and Design*, vol. 232, no. 2, pp. 197–216, 2004.

[3] Y. Wang, "Preliminary study for the passive containment cooling system analysis of the advanced PWR," *Energy Procedia*, vol. 39, pp. 240–247, 2013.

[4] Z. Liu, B. Sunden, and J. Yuan, "VOF modeling and analysis of filmwise condensation between vertical parallel plates," *Heat Transfer Research*, vol. 43, no. 1, pp. 47–68, 2012.

[5] X. Ma, S. Wang, Z. Lan, B. Peng, H. B. Ma, and P. Cheng, "Wetting mode evolution of steam dropwise condensation on superhydrophobic surface in the presence of noncondensable gas," *Journal of Heat Transfer*, vol. 134, no. 2, Article ID 021501, 2012.

[6] X. Chen, J. Wu, R. Ma et al., "Nanograssed micropyramidal architectures for continuous dropwise condensation," *Advanced Functional Materials*, vol. 21, no. 24, pp. 4617–4623, 2011.

[7] C.-H. Chen, Q. Cai, C. Tsai et al., "Dropwise condensation on superhydrophobic surfaces with two-tier roughness," *Applied Physics Letters*, vol. 90, no. 17, Article ID 173108, 2007.

[8] J. W. Rose, "Dropwise condensation theory and experiment: a review," *Proceedings of the Institution of Mechanical Engineers, Part A: Journal of Power and Energy*, vol. 216, no. 2, pp. 115–128, 2002.

[9] K. B. Blodgett, "Films built by depositing successive monomolecular layers on a solid surface," *Journal of the American Chemical Society*, vol. 57, no. 6, pp. 1007–1022, 1935.

[10] G. Koch, K. Kraft, and A. Leipertz, "Parameter study on the performance of dropwise condensation," *Revue Générale de Thermique*, vol. 37, no. 7, pp. 539–548, 1998.

[11] W. Zhao, R.-Z. Wang, Z.-W. Song, H. Wang, H. Yan, and P. K. Chu, "Crystallization effects of nanocrystalline GaN films on field emission," *Journal of Physical Chemistry C*, vol. 117, no. 3, pp. 1518–1523, 2013.

[12] C. J. Glassbrenner and G. A. Slack, "Thermal conductivity of silicon and germanium from 3°K to the melting point," *Physical Review*, vol. 134, no. 4, Article ID A1058, 1964.

[13] S.-H. Huang, J. Liu, W.-K. Jing, F. Lu, and G.-J. Hu, "Fabrication and electrical properties of polycrystalline Si films on glass substrates," *Materials Research Bulletin*, vol. 49, no. 1, pp. 71–75, 2014.

[14] K.-H. Chu, R. Xiao, and E. N. Wang, "Uni-directional liquid spreading on asymmetric nanostructured surfaces," *Nature Materials*, vol. 9, no. 5, pp. 413–417, 2010.

[15] J. Drelich, E. Chibowski, D. D. Meng, and K. Terpilowski, "Hydrophilic and superhydrophilic surfaces and materials," *Soft Matter*, vol. 7, no. 21, pp. 9804–9828, 2011.

[16] F. Zhang, W. B. Zhang, Z. Shi, D. Wang, J. Jin, and L. Jiang, "Nanowire-haired inorganic membranes with superhydrophilicity and underwater ultralow adhesive superoleophobicity for high-efficiency oil/water separation," *Advanced Materials*, vol. 25, no. 30, pp. 4192–4198, 2013.

[17] R. N. Wenzel, "Resistance of solid surfaces to wetting by water," *Industrial & Engineering Chemistry*, vol. 28, no. 8, pp. 988–994, 1936.

[18] R. N. Wenzel, "Surface roughness and contact angle," *The Journal of Physical & Colloid Chemistry*, vol. 53, no. 9, pp. 1466–1467, 1949.

[19] A. B. D. Cassie and S. Baxter, "Wettability of porous surfaces," *Transactions of the Faraday Society*, vol. 40, pp. 546–551, 1944.

[20] C. Sendner, D. Horinek, L. Bocquet, and R. R. Netz, "Interfacial water at hydrophobic and hydrophilic surfaces: slip, viscosity, and diffusion," *Langmuir*, vol. 25, no. 18, pp. 10768–10781, 2009.

[21] K. Liu, M. Cao, A. Fujishima, and L. Jiang, "Bio-inspired titanium dioxide materials with special wettability and their applications," *Chemical Reviews*, vol. 114, no. 19, pp. 10044–10094, 2014.